Biomimetics

DOI: 10.1002/anie.201301850

Redox Cofactor from Biological Energy Transduction as Molecularly Tunable Energy-Storage Compound**

Minah Lee, Jihyun Hong, Dong-Hwa Seo, Dong Heon Nam, Ki Tae Nam, Kisuk Kang, and Chan Beum Park**

Energy transduction and storage in biological systems involve multiply coupled, stepwise reduction/oxidation of energy-carrying molecules such as adenosine triphosphate (ATP), nicotinamide, and flavin cofactors.[1,2] These are synthesized as a result of oxidation during citric acid cycles in mitochondria or during photosynthesis in chloroplasts, and high energies stored in their chemical bonds are consequently harnessed for many biological reactions.[3,4] Phosphorylation and protonation are key underlying mechanisms that allow for reversible cycling and regulate the molecule-specific redox potential.[5] A sequential progression of electron transfer through the redox cascades as well as continuous recycling of the redox centers enables efficient energy use in biological systems.[6,7]

The biological energy transduction mechanism hints at the construction of a man-made energy storage system.[8] Since the pioneering work by Tarascon and co-workers[9] towards a sustainable lithium rechargeable battery received significant resonance, organic materials such as carbonyl, carboxy, or quinone-based compounds have been demonstrated to be bio-inspired organic electrodes.[10–14] The imitation of redox-active plastoquinone and ubiquinone cofactors[15] through the use of redox-active C=O functionalities in organic electrodes is a significant step forward to biomimetic energy storage. However, the biological energy transduction is based on numerous redox centers of versatile functionalities available in nature, not limited to the simple redox active C=O functionalities. Consideration of how natural energy transduction systems function at organelle or cellular levels by elucidating the basic components and their operating principles selected by evolution[16] will enrich the biomimetic strategy for efficient and green energy storage.

Flavins are one of most structurally and functionally versatile redox centers in nature, catalyzing an enormous range of biotransformations and electron-transfer reactions,[17,18] which occur over a wide potential range (>500 mV).[19,20] The extraordinary versatility of flavins stems from their ability to engage in either one- or two-electron-transfer redox processes, accompanying proton transfer at the nitrogen atoms of diazabutadiene motif. In the respiratory electron transport chain, for example, electrons from reduced flavin adenine dinucleotide ($FADH_2$) are transported along a group of proteins located in the inner membrane of mitochondria to induce proton pumping across the membrane, as illustrated in Figure 1a (left). This process generates an electrochemical proton gradient, which results in the formation of high-energy ATP.[21] FAD is reduced again in the citric acid cycle of mitochondria, which enables continuous recycling of flavin redox centers. A close analogy exists between the key components, facilitating respiration and battery operation (Figure 1a); charged ions (H^+ or Li^+) and electrons, which are derived from flavin redox centers, are unidirectionally transported in a stoichiometric manner using separated paths. This creates chemical gradients across membranes, and finally results in the formation of high-energy species such as ATP and metallic lithium.

Herein, we report on the possibility of using the energy-storage mechanism of flavin redox cycling in mitochondria to lithium rechargeable batteries. According to our results, flavin electrodes were capable of reversibly storing and releasing two lithium ions and two electrons per formula unit. Redox reactions in flavin electrodes were thoroughly investigated using the combined analyses of ex situ characterizations and density functional theory (DFT)-based calculations. We found that the flavin redox reaction occurs during battery operation at the nitrogen atoms of the diazabutadiene motif in flavin molecules using two successive single-electron transfer steps, in a similar way to the proton-coupled electron transfer in flavoenzymes. Molecular tuning by chemical substitution on the isoalloxazine ring significantly improved electrochemical performances in terms of an average redox potential, a gravimetric capacity, and stability, resulting in a high-energy density comparable to that of $LiFePO_4$, the

[*] M. Lee,[+] D. H. Nam, Prof. C. B. Park
Department of Materials Science and Engineering
Korea Advanced Institute of Science and Technology
Daejeon 305-701 (Korea)
E-mail: parkcb@kaist.ac.kr

J. Hong,[+] Dr. D.-H. Seo, Prof. K. T. Nam, Prof. K. Kang
Center for Nanoparticle Research
Institute for Basic Science (IBS)
Department of Materials Science and Engineering
Research Institute of Advanced Materials
Seoul National University, Seoul 151-742 (Korea)
E-mail: matlgen1@snu.ac.kr

[+] These authors contributed equally to this work.

[**] This work was supported from the National Research Foundation (NRF) grants by the Korea government (MEST) (National Leading Research Laboratory Program, R0A-2008-000-20041-0; Intelligent Synthetic Biology Center of Global Frontier Project, 2011-0031957; NRF-2009-0094219). It was also supported by Human Resources Development of the Korea Institute of Energy Technology Evaluation and Planning (KETEP) grant funded by the Korea government Ministry of Knowledge Economy (grant number 20114010203120). K.K is grateful to the Korea Institute of Science and Technology Information for providing supercomputing resources.

Supporting information for this article is available on the WWW under http://dx.doi.org/10.1002/anie.201301850.

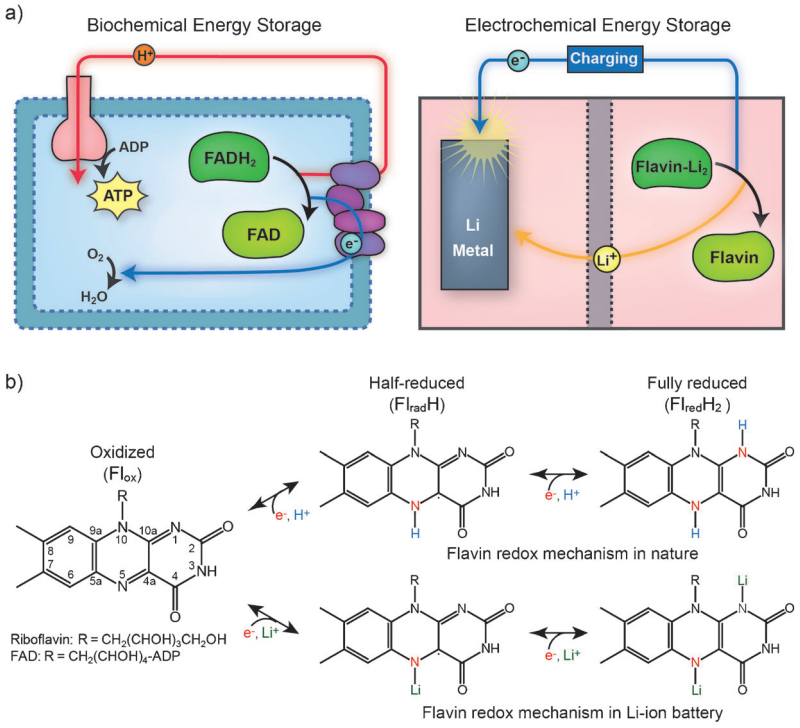

Figure 1. a) Energy transduction in mitochondria (left panel) where flavins work as a redox center to store energy from nutrients into high-energy ATP. For synthetic energy device applications (right panel), flavins serve as an active material that reversibly takes up and releases electrons and lithium ions during electrochemical energy storage. b) Different redox states of flavin molecules with indications of redox-active parts upon electron uptake. Flavin molecules conduct a proton-coupled electron transfer reaction at N5 and N1 in nature (top). We suggest the flavin redox cycle can be applied to lithium rechargeable batteries using the reaction scheme proposed (bottom).

well-known inorganic cathode material for lithium rechargeable batteries.

Flavins (Fls) can take up and release lithium ions reversibly through a similar mechanism that occurs in biological systems (Figure 1b). They possess three oxidation states: oxidized (Fl_{ox}), half-reduced ($Fl_{rad}H$), and fully reduced ($Fl_{red}H_2$) states (Figure 1b, top).[22] The main loci of redox reactivity in the 7,8-dimethylisoalloxazine ring of the flavin molecules are nitrogen atoms at positions N1 and N5. The reduction and oxidation within the N5-C4a-C10a-N1 region enable the cycling between these three oxidation states.[23] The quinone groups in flavins do not function as redox-active site, but only participate in the intermolecular hydrogen bonding.[24] We tested the electrochemical activity of a riboflavin electrode versus lithium in a conventional coin-type cell. Riboflavin (also known as vitamin B_2) is a biochemical source for the redox-active moiety of flavin cofactors. According to our galvanostatic measurements, riboflavin/Li cells exhibited a reversible capacity of approximately 105.89 mA h g^{-1}, equivalent to 1.49 Li atoms per unit formula between 1.5 and 3.8 V at a current rate of 10 mA g^{-1} (Figure 2a). The theoretical capacity of two lithium ions in the riboflavin electrode is 142.43 mA h g^{-1}. We also conducted galvanostatic intermittent titration technique (GITT) measurements with the riboflavin electrode under a low current density, which allowed sufficient time for full lithium access to riboflavin (Figure 2a, inset). Based on the GITT result, which manifests a much higher reversible capacity (1.90 Li atoms per riboflavin molecule), it is demonstrated that the flavin electrode is capable of accepting and releasing two lithium ions per formula unit, as proposed in Figure 1b (bottom).

The energy storage reaction of the riboflavin electrode was found to follow two consecutive one-electron transfer reactions. The differential capacity curves contain two sets of distinctive cathodic and anodic peaks with average potentials of 2.65 and 2.4 V, respectively (Figure 2b). This indicates that the lithium-coupled electron-transfer reaction of the riboflavin electrode occurs in two different environments and evidences a relative stability of the intermediate phase, resulting in two consecutive one-electron reduction steps, as depicted in Figure 2c (left). The first reduction ($E_{ox/rad}$) by lithiation (that is, acceptance of lithium in the molecule) of riboflavin yields a stable intermediate phase: lithiated flavosemiquinone ($Fl_{rad}Li$). It is followed by the second reduction ($E_{rad/red}$) to form a fully lithiated flavoquinone ($Fl_{red}Li_2$). This is in clear contrast to free flavins dissolved in aqueous (or protic organic) media, where the flavoquinone (Fl_{ox}) is reduced directly into flavohydroquinone ($Fl_{red}H_2$) through a two-electron and two-proton transfer process in Figure 2c (right).[25–27] The difference between the lithium-derived two-step reaction and the one-step reaction in the protonation of free flavin molecules will be discussed later with the DFT calculations, and further discussion is in Section 3 of the Supporting Information.

To unveil the mechanism of flavin redox reaction with lithium, we have analyzed the riboflavin electrodes during battery operation by using ex situ XPS at 1) as-prepared, 2) fully discharged, and 3) fully recharged states. In the high-resolution XPS scans of riboflavin electrodes (Figure 3a), lithium insertion and deinsertion were clearly observed. Li 1s spectra indicate the evolution of the lithium peak for the discharged electrode stemming from the lithium insertion into riboflavin. Upon recharge, the lithium peak substantially reduces as lithium is extracted from the riboflavin. The reversible lithium insertion and deinsertion also affect the bonding of nitrogen and oxygen in riboflavin. N 1s spectra show that the peak was noticeably broadened with lithium insertion (that is, discharged) and restored as lithium was extracted. For the as-prepared electrode, the N 1s spectrum initially fits well with two peaks having the same full width at half maximum (FWHM; 1.8 eV) centered at 400.2 and 401.4 eV. They are assigned to conjugated (sp^2) -N= and non-conjugated (sp^3) -NH- groups, respectively.[28,29] For the discharged electrode, peak broadening occurs because of an additional peak at 399 eV, implying the formation of a new bond between nitrogen and lithium. The peak centered at about 399 eV in the N 1s region was designated as an N-Li

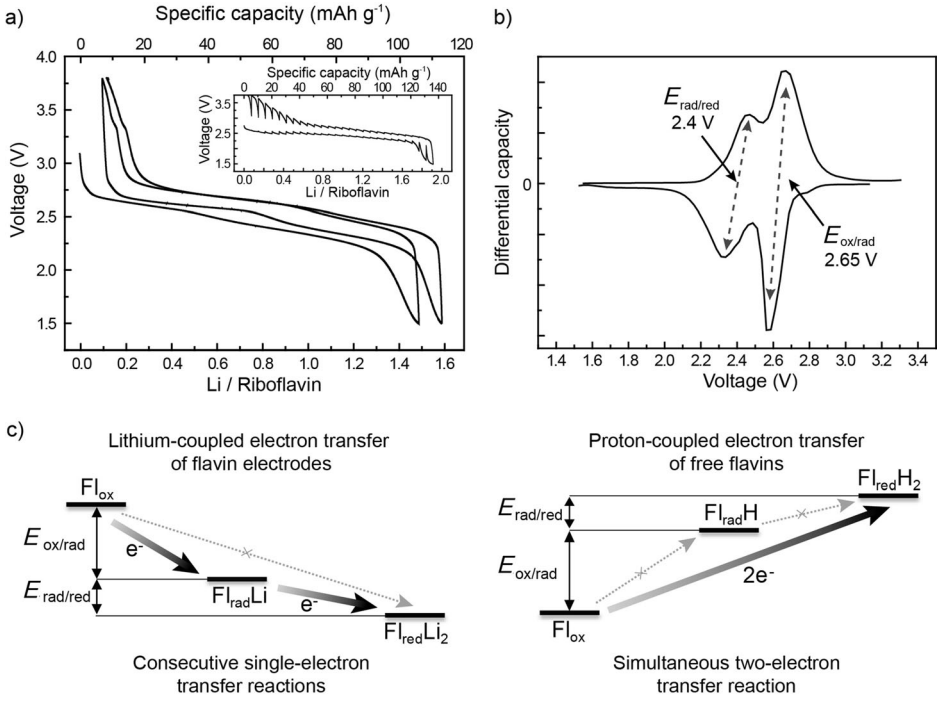

Figure 2. a) Discharge/charge profiles of a Li/riboflavin cell and GITT profiles (inset). b) Differential capacity (*dQ/dV*) curves of a Li/riboflavin cell calculated from the data shown in (a) indicating two consecutive one-electron transfer reactions. c) Thermodynamic energy states of flavin (Fl) electrodes and free flavin molecules during reduction indicating different electron-transfer pathways. The thick arrows correspond to the actual reaction path, whereas the dotted arrows represent the infeasible path.

bond similar to that in lithium azide.[30,31] The variation of the -N = peak (400.2 eV) intensity with respect to the -NH- peak (401.4 eV) also indicates reduction and oxidation of the riboflavin, although the limited resolution of N 1s did not allow a quantitative analysis. The reversible reduction of the N-Li peak at 399 eV as well as the recovery of the -N = peak in the recharged electrode coincides with the redox reaction of riboflavin with lithium. The O 1s peak also varied during lithium insertion/extraction. The shift of the O 1s band toward lower binding energy in the discharged electrode suggests an increase in electron density of oxygen atoms accompanied by lithiation of riboflavin during the discharge step.[32,33]

The change in the bonding nature of riboflavin after the lithium-coupled reduction was further observed by ex situ FTIR analysis (Figure 3b). With charge and discharge, the absorbance signals at 1580, 1547, and 1511 cm^{-1} from the vibrational modes of C=N double bonds in riboflavin [ν-(C4a=N5) and ν(C10a=N1)][34,35] significantly change, indicating the participation of C=N double bonds in the reaction with lithium. This strongly supports the formation of a N-Li bond. Additionally, we found a reversible change in the C=O vibrational mode [ν(C2=O2) and ν(C4=O4)],[34] which indicates that C=O double bonds also participate in the reaction with lithium during charge and discharge. This observation is in contrast to the case of $Fl_{red}H_2$, in which the redox reaction only occurs at C=N double bonds. This discrepancy will be discussed in the DFT calculations below. Additional evidence of reversible lithium reaction with riboflavin, such as spectrophotometry and ^{6}Li NMR analysis, is provided in the Supporting Information.

We conducted the density-functional theory (DFT) calculations (B3LYP) for in-depth understanding of our experimental results. To verify the plausibility of lithium insertion, various possible lithium sites were examined in the riboflavin (see Figure S4 in the Supporting Information). We found that the first lithium (Li1) insertion occurs via the formation of the N5-Li1 bond of riboflavin (Figure 3c). The N5-Li1 bond was more stable than other bonds, such as N1-Li1, by 576 meV, which is significantly large considering the thermal energy at room temperature (about 25 meV). This result is consistent with the proton-coupled electron transfer of flavins, where the first proton binds to N5.[36] Subsequently, lithium binds to the remaining N1 atom, forming $Fl_{red}Li_2$ during the following reduction procedure. Based on the formation energy, the chemical potentials of lithium in riboflavin after the first and the second lithium insertions were estimated to be 3.1 eV ($\Delta E_{ox/rad}$) and 2.4 eV ($\Delta E_{rad/red}$), respectively; although the values are slightly different from the experimental observation because of possible intermolecular interactions, such as hydrogen bonding and aromatic stacking, the trend of chemical potential changes along de/lithiation processes is reasonable. While the main bonding occurs between lithium and nitrogen, lithium also interacts with oxygen because of the comparatively large size of the lithium ion (59 pm).[37] Thus, the first lithium insertion induces the formation of a heterocyclic five-membered -C4a-C4-O4-Li1-N5-C4a- ring, whereas the next lithium insertion creates a four-membered ring: -C2-N1-Li2-O2-C2-. The geometrically strained four-membered ring is much less stable than the five-membered ring system, so that the energy state of $Fl_{red}Li_2$ becomes higher. Therefore, the relative stability of the intermediate $Fl_{rad}Li$ phase results in two consecutive electron-transfer reactions, which is in agreement with our electrochemical data.

The changes in the major bond lengths obtained from DFT calculation (Figure 3d) clearly manifest the change of bonding nature of conjugated diazabutadiene in 7,8-dimethylisoalloxazine ring during the redox reaction of riboflavin electrode. Upon lithiation, asymmetric bonding of = N5- and = N1- was successively converted into symmetric -*N*- with an increase in the length of the C=N double bond, indicating the reduction of the double bond. In addition, in the fully reduced state of riboflavin, the distance between C4a and C10 was shortened, implying the oxidation of a single bond to a double bond. A slight increase in the C=O double-bond lengths was

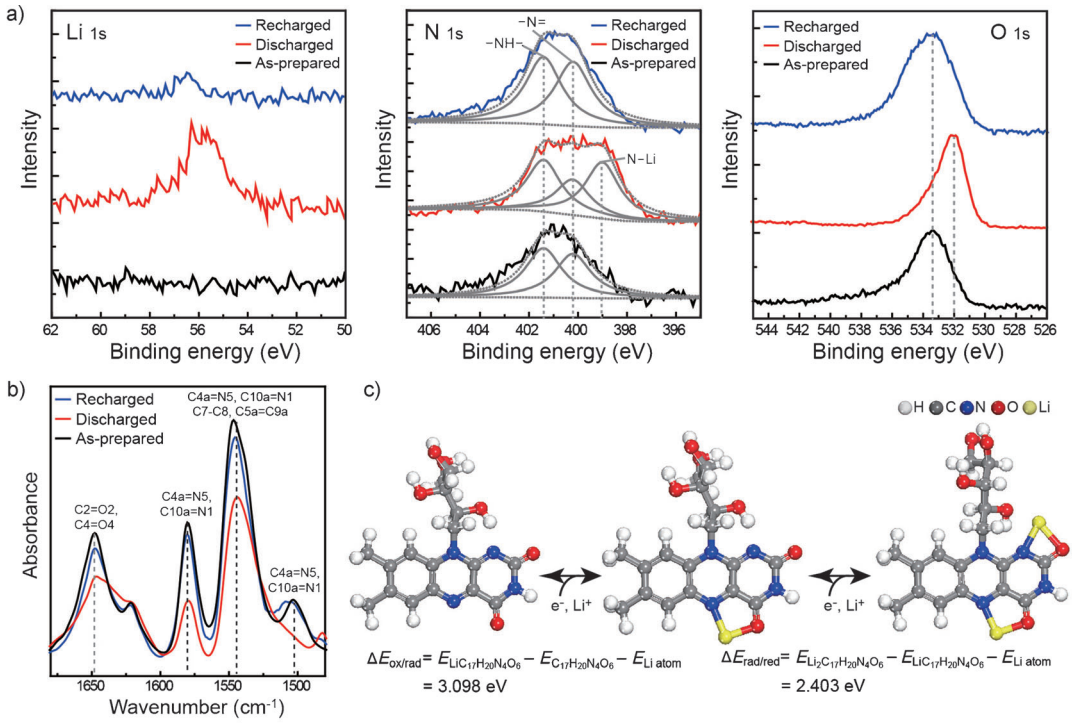

d)

	N5=C4a (1)	N5-C5a (2)	(1) - (2)	N1=C10a (3)	N1-C2 (4)	(3) - (4)	C4a-C10a	C4=O	C2=O
Fl_{ox}	1.29556	1.36337	0.06781	1.30924	1.38264	0.0734	1.45211	1.21001	1.21205
$Fl_{rad}Li$	1.36603	1.36780	0.00177	1.32468	1.36864	0.04396	1.41564	1.26504	1.21671
$Fl_{red}Li_2$	1.39381	1.37384	-0.01997	1.34652	1.34336	-0.00316	1.38449	1.26836	1.26532

Figure 3. a,b) Ex situ characterizations of the riboflavin electrodes at different states of charge: as-prepared state (black), fully discharged state (1.5 V, red), and fully recharged state (3.8 V, blue). XPS local scan spectra of Li 1s, N 1s, and O 1s regions (a). FTIR spectra containing information of CN and CO bonds (b). c) Molecular structure of riboflavin upon lithium insertion, predicted from DFT calculations. d) The major bond lengths (Å) measured from the data shown in (c). With lithium uptake, consecutive bond-length alternation in the N5-C4a-C10a-N1 region is observed, indicating reduction.

observed, which is compatible with other experimental and computational results. Furthermore, the redox-active sites upon electron uptake were identified by calculating the Mulliken charges of atoms in riboflavin (Figure S5). The notable increase in the electron density of oxygen atoms implies that the oxygen atoms also partially participate in the redox reaction, whereas nitrogen atoms play a role as major redox centers in the molecule. Overall, DFT calculations support our experimental observations of the reversible mechanism of the lithium-coupled electron transfer reaction of riboflavin.

Taking the benefit of chemical tunability of organic materials, we have designed tailored flavin derivatives that exhibit much improved electrochemical properties in terms of energy density and cyclability as shown in Figure 4a. In nature, a number of flavin analogs exist with different substituents on the isoalloxazine ring, which show different electrochemical properties in diverse biological redox events.[38] As a bioinspired strategy, we considered the following criteria of molecular substitutions in the design of organic electrode: 1) substituents with stronger electron-withdrawing properties in the benzene subnucleus (C7 and C8) to elevate the redox potential, 2) simpler side chains at the N10 site to increase the gravimetric capacity, and 3) functionalities with low polarity to inhibit the dissolution of active materials.

According to our results (Figure 4b), the replacement of the methyl group by chlorine atoms at C7 and C8 (7,8-dichloro-10-ribitylisoalloxazine), and bromine atom at C8 (7-methyl-8-bromo-10-ribitylisoalloxazine) raised the operating voltage of flavin electrodes. The changes in the average redox potential for each analog were 0.14 and 0.09 V, respectively. We expect a substitution with much stronger electron-withdrawing groups, such as cyano,[38] will enable further elevation of the redox potential of flavins. The replacement of the ribityl group at N10 in riboflavin with a methyl group can lead to a simpler molecule, called lumiflavine (Figure 4a), with a theoretical capacity as high as 209.18 mA h g^{-1}. According to our observation, the gravimetric capacity of lumiflavine was much higher (174.32 mA h g^{-1}) than that of riboflavin (105.88 mA h g^{-1}) with negligible transition in the redox potential in a galvanostatic measurement under the same

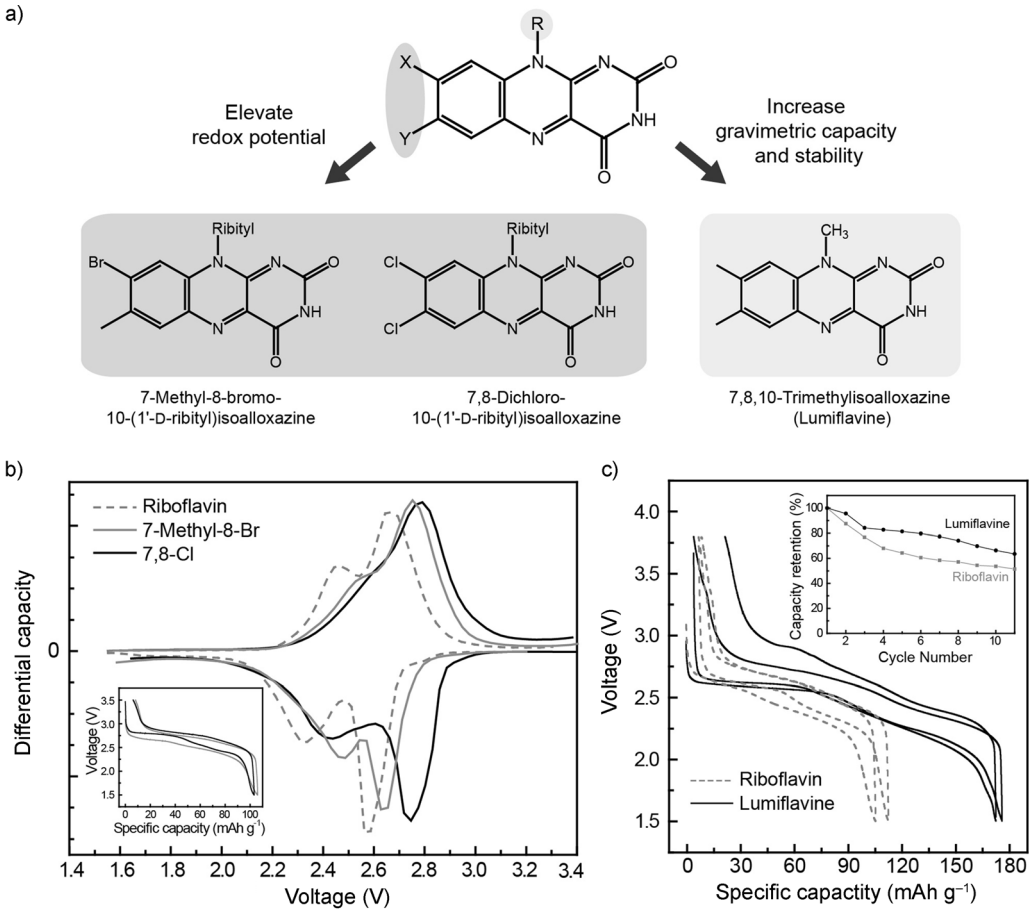

Figure 4. Design of flavin molecules to enhance electrochemical performances. a) Chemical structures of tailored flavin derivatives. b) Differential capacity (dQ/dV) curves of Li/7-methyl-8-bromo-10-(1′-D-ribityl)isoalloxazine (gray) and Li/7,8-dichloro-10-(1′-D-ribityl)isoalloxazine (black) cells compared to Li/riboflavin cell (gray, dotted) calculated from the discharge/charge profiles (inset). c) Discharge/charge profiles of a Li/lumiflavine cell (black) compared to the Li/riboflavin cell (gray, dotted). The capacity retention of the Li/lumiflavine cell compared to the Li/riboflavin cell is shown in the inset.

experimental conditions. In addition, the alternation of the side group from ribityl to nonpolar group reduced dissolution of flavin molecules in polar electrolytes.[36] The lumiflavine electrode exhibited the capacity retention of 66.3% after 10 cycles, which is higher than that of the riboflavin electrode (53.6%; Figure 4c inset). We attribute this result to the differential solubility of the molecules. For practical applications, the stability of flavin electrodes should further be improved by adopting engineering options, such as polymerization or immobilization and the use of a solid-state electrolyte. Beside the substituents, molecular conformation as well as intermolecular interactions, such as hydrogen bonding and aromatic stacking, also contribute to the redox properties of flavins,[24] and should therefore be taken into account when designing a tailored flavin electrode.

In summary, this work demonstrates a biomimetic approach to design high-performance energy devices based on the analogy between energy-storage phenomena of mitochondria and lithium rechargeable batteries. We found that flavins such as vitamin B_2 and lumiflavine are capable of reversibly storing lithium by using redox-active nitrogen atoms in the diazabutadiene motif during battery operation. Analyses of both ex situ characterizations and DFT calculations revealed that electron transfer reactions in the flavin electrode during lithium-coupled electron uptake and donation are analogous to the proton-coupled electron transfer mechanism of flavoenzymes. Proper chemical modification of flavin molecules can improve battery performances; applying strong, electron-withdrawing substituents at the benzene subnucleus and a simple side chain at the pyrazine subnucleus of the isoalloxazine ring, the energy density of the flavin cathode (i.e. 510 $Wh\,kg^{-1}$ for lumiflavine) can compete with that of the commercial inorganic electrode material, $LiFePO_4$, while more study is required to have lithiated compounds and to overcome the intrinsic low volumetric density of the organic materials. These findings confirm that natural living systems, which have become optimized for energy cycling through evolution, hint at unlimited opportunities for us to design sustainable materials with a superior performance beyond the conventional electrodes in lithium rechargeable batteries.

Experimental Section

Electrochemical measurements: Electrochemical performances of flavin molecules were measured versus a Li metal foil (Hohsen Corp.,

Japan) in coin-type cells (CR2016). The electrodes were fabricated by mixing 50% w/w active materials, 30% w/w carbon black (Super P®) and 20% w/w PTFE (polytetrafluoroethylene, Aldrich) binder. A porous polypropylene membrane (Celgard 2400) was used as a separator. The electrolyte was 1M $LiPF_6$ in ethylene carbonate (EC)/dimethyl carbonate (DMC) (1:1 v/v, Techno Semichem Co., Ltd., Korea). The cells were assembled in an inert atmosphere within an Ar-filled glove box. The discharge and charge measurements were carried out at a constant current density of 10 mA g^{-1} in voltage ranges of 1.5–3.8 V on a battery test system (Won-A Tech, Korea). For GITT measurement, the Li/flavin cells were discharged and charged for 1 h at 5 mA g^{-1}, with 2 h rest time, in galvanostatic mode.

Confirmation of the material stability: To confirm structural consistency, X-ray diffraction (XRD) patterns of riboflavin powder and the as-prepared riboflavin electrode were collected on a Bruker D2phaser (Germany) using Cu Kα radiation ($\lambda = 1.54178$ Å) with a scanning speed of 1° per minute in the range $2\theta_{Cu\,K\alpha} = 5$–40° with a 2θ step size of 0.02°. The photochemical stability of the riboflavin electrode with electrolyte EC/DMC was confirmed by Fourier transform infrared spectroscopy (FTIR) and UV/Vis absorbance spectroscopy. The riboflavin powder, as-prepared electrodes, and as-prepared electrodes stored in EC/DMC for 24 h were compared. The electrode retrieved by disassembling as-prepared coin cells preserved for 24 h and rinsed with DMC was used as the sample stored in electrolyte. FTIR spectra of pellets made of riboflavin powder (or electrodes) and KBr powder were recorded on a FT/IR-4200 (Jasco Inc., Japan) at a resolution of 2 cm^{-1} in argon atmosphere. For UV/Vis absorbance spectroscopy, each sample was immersed in degassed, deionized water in argon atmosphere, resulting in immediate solubilization of the riboflavin molecules. UV/Vis absorbance spectra were obtained using a V/650 spectrophotometer (Jasco Inc., Japan) in the range of 200–600 nm.

Ex situ electrode characterization: For ex situ analyses, the electrodes at the different states of charge (as-prepared, fully discharged to 1.5 V, and fully recharged to 3.8 V) were disassembled from coin cells and rinsed with DMC. To prevent exposure to air, all the samples were handled in an Ar-filled glove box. X-ray photoelectron spectroscopy (XPS) measurements were performed by using a Thermo VG Scientific Sigma Probe spectrometer (U.K.) equipped with a microfocus monochromated X-ray source (90 W). All the binding energies are referenced to C 1s (284.5 eV). FTIR and absorbance spectra were collected by following the method described previously in stability confirmation. ^{6}Li magic-angle spinning (MAS) nuclear magnetic resonance (NMR) analysis was performed for the riboflavin electrode after fully discharged to 1.5 V. The NMR spectrum was obtained using a solid-state 400 MHz NMR spectrometer (AVANCE 400WB, Bruker Science, Germany) at room temperature.

Computational details: All energy calculations were conducted with spin-unrestricted density functional theory (DFT) using the Gaussian 09 quantum chemistry package.[39] Geometry optimizations were carried out with Becke–Lee–Yang–Parr (B3LYP) hybrid exchange-correlation functional[40,41] and the standard TZVP basis set.[42–44] To determine the sites and sequence of lithium occupation upon redox reactions, DFT energies of various possible forms of $Fl_{rad}Li$ and $Fl_{red}Li_2$ were compared. Mulliken population analysis was used to analyze atomic charge.[45] The detailed procedure and results of DFT calculations are discussed in the Supporting Information.

Received: March 5, 2013
Published online: June 19, 2013

Keywords: bioenergetics · biomimetics · flavins · lithium battery · organic electrodes

[1] J. F. Allen, W. Martin, *Nature* **2007**, *445*, 610–612.
[2] J. Piera, J.-E. Backvall, *Angew. Chem.* **2008**, *120*, 3558–3576; *Angew. Chem. Int. Ed.* **2008**, *47*, 3506–3523.
[3] M. Hervás, J. A. Navarro, M. A. De La Rosa, *Acc. Chem. Res.* **2003**, *36*, 798–805.
[4] G. Cecchini, *Annu. Rev. Biochem.* **2003**, *72*, 77–109.
[5] M. Saraste, *Science* **1999**, *283*, 1488–1493.
[6] C. C. Page, C. C. Moser, X. Chen, P. L. Dutton, *Nature* **1999**, *402*, 47–52.
[7] A. Osyczka, C. C. Moser, F. Daldal, P. L. Dutton, *Nature* **2004**, *427*, 607–612.
[8] P. Yang, J. M. Tarascon, *Nat. Mater.* **2012**, *11*, 560–563.
[9] H. Chen, M. Armand, G. Demailly, F. Dolhem, P. Poizot, J. M. Tarascon, *ChemSusChem* **2008**, *1*, 348–355.
[10] H. Chen, M. Aramnd, M. Courty, M. Jiang, C. P. Grey, F. Dolhem, J. M. Tarascon, P. Poizot, *J. Am. Chem. Soc.* **2009**, *131*, 8984–8988.
[11] Z. Song, H. Zhan, Y. Zhou, *Chem. Commun.* **2009**, 448–450.
[12] M. Armand, S. Grugeon, H. Vezin, S. Laruelle, P. Ribière, P. Poizot, J. M. Tarascon, *Nat. Mater.* **2009**, *8*, 120–125.
[13] R. Zeng, X. Li, Y. Qiu, W. Li, J. Yi, D. Lu, C. Tan, M. Xu, *Electrochem. Commun.* **2010**, *12*, 1253–1256.
[14] M. Yao, H. Senoh, S.-I. Yamazaki, Z. Siroma, T. Sakai, K. Yasuda, *J. Power Sources* **2010**, *195*, 8336–8340.
[15] P. Poizot, F. Dolhem, *Energy Environ. Sci.* **2011**, *4*, 2003–2019.
[16] V. I. Vullev, *J. Phys. Chem. Lett.* **2011**, *2*, 503–508.
[17] A. O. Cuello, C. M. McIntosh, V. M. Rotello, *J. Am. Chem. Soc.* **2000**, *122*, 3517–3521.
[18] G. Kurisu, M. Kusunoki, E. Katoh, T. Yamazaki, K. Teshima, Y. Onda, Y. Kimata-Ariga, T. Hase, *Nat. Struct. Biol.* **2001**, *8*, 117–121.
[19] V. Joosten, W. J. van Berkel, *Curr. Opin. Chem. Biol.* **2007**, *11*, 195–202.
[20] R. Miura, *Chem. Rec.* **2001**, *1*, 183–194.
[21] P. Kakkar, B. K. Singh, *Mol. Cell. Biochem.* **2007**, *305*, 235–253.
[22] S. L. J. Tan, R. D. Webster, *J. Am. Chem. Soc.* **2012**, *134*, 5954–5964.
[23] G. Wille, M. Ritter, R. Friedemann, W. Mantele, G. Hubner, *Biochemistry* **2003**, *42*, 14814–14821.
[24] E. Breinlinger, A. Niemz, V. M. Rotello, *J. Am. Chem. Soc.* **1995**, *117*, 5379–5380.
[25] B. Janik, P. J. Elving, *Chem. Rev.* **1968**, *68*, 295–319.
[26] A. M. Hartley, G. S. Wilson, *Anal. Chem.* **1966**, *38*, 681–687.
[27] H. Wei, S. Omanovic, *Chem. Biodiversity* **2008**, *5*, 1622–1639.
[28] J. Peeling, F. E. Hruska, N. S. Cintyre, *Can. J. Chem.* **1978**, *56*, 1555–1561.
[29] G. Bhargava, T. A. Ramanarayanan, S. L. Bernasek, *Langmuir* **2010**, *26*, 215–219.
[30] J. Sharma, T. Gora, J. D. Rimstidt, R. Staley, *Chem. Phys. Lett.* **1972**, *15*, 232–235.
[31] T. H. Lee, R. J. Colton, M. G. White, J. W. Rabalais, *J. Am. Chem. Soc.* **1975**, *97*, 4845–4851.
[32] J. C. Dupin, D. Gonbeau, P. Vinatierb, A. Levasseur, *Phys. Chem. Chem. Phys.* **2000**, *2*, 1319–1324.
[33] G. Pacchioni, P. S. Bagus, *Phys. Rev. B* **1994**, *50*, 2576–2581.
[34] M. M. N. Wolf, C. Schumann, R. Gross, T. Domratcheva, R. Diller, *J. Phys. Chem. B* **2008**, *112*, 13424–13432.
[35] M. Takahashi, Y. Ishikawa, J. Nishizawa, H. Ito, *Chem. Phys. Lett.* **2005**, *401*, 475–482.
[36] A. Niemz, J. Imbriglio, V. M. Rotello, *J. Am. Chem. Soc.* **1997**, *119*, 887–892.
[37] R. D. Shannon, *Acta Crystallogr. Sect. A* **1976**, *32*, 751–767.
[38] J. J. Hasford, W. Kemnitzer, C. J. Rizzo, *J. Org. Chem.* **1997**, *62*, 5244–5245.

[39] Gaussian 09, Revision A.02, M. J. Frisch, G. W. Trucks, H. B. Schlegel, G. E. Scuseria, M. A. Robb, J. R. Cheeseman, G. Scalmani in no. 3 Gaussian. Inc., Wallingford, **2009**, 4.
[40] C. Lee, W. Yang, R. G. Parr, *Phys. Rev. B* **1988**, *37*, 785 – 789.
[41] A. D. Becke, *J. Chem. Phys.* **1993**, *98*, 5648 – 5652.
[42] A. Schaefer, H. Horn, R. Ahlrichs, *J. Chem. Phys.* **1992**, *97*, 2571 – 2577.
[43] A. Schaefer, C. Huber, R. Ahlrichs, *J. Chem. Phys.* **1994**, *100*, 5829 – 5835.
[44] B. Klaumünzer, D. Kroner, P. Saalfrank, *J. Phys. Chem. B* **2010**, *114*, 10826 – 10834.
[45] R. S. Mulliken, *J. Chem. Phys.* **1955**, *23*, 1833 – 1840.

